CrossMark

# The mass spectra and decay properties of dimesonic states, using the Hellmann potential

**Ajay Kumar Rai**[a], **D. P. Rathaud**

Department of Applied Physics, Sardar Vallabhbhai National Institute of Technology, Surat 395007, Gujarat, India

**Abstract** Mass spectra of the dimesonic (meson–antimeson) molecular states are computed using the Hellmann potential in a variational approach, which consists of a relativistic correction to the kinetic energy term as well as to the potential energy term. For the study of a molecular bound state system, the Hellmann potential, of the form $V(r) = -\frac{\alpha_s}{r} + \frac{Be^{-Cr}}{r}$, is being used. The one pion exchange potential is also incorporated in the mass calculation. The digamma decay width and decay width of the dimesonic system are evaluated using the wave function. The experimental states such as $f_0(980)$, $b_1(1235)$, $h_1(1380)$, $a_0(1450)$, $f_0(1500)$, $f_2'(1525)$, $f_2(1565)$, $h_1(1595)$, $a_2(1700)$, $f_0(1710)$ and $f_2(1810)$ are compared with dimesonic states. Many of these states (masses and their decay properties) are close to our theoretical predictions.

## 1 Introduction

The spectroscopy of hadrons imparts information of a basic force of nature. The theory of Quantum Chromo Dynamics (QCD) is a tool to understand the strong force in which hadron spectroscopy plays a key role in the non-perturbative and the perturbative regime. The new experimental developments at Belle, BES, CLEO, CDF, LHC, BABAR brought out enormous data and came with large numbers of surprises [1–5]. A number of new states are observed which do not fit in the conventional $q\bar{q}$ scheme, mainly in the meson sector. All these exotic states which do not fit in qqq and $q\bar{q}$ schemes require extra theoretical attention [6–13].

Recently, in partial wave analysis (PWA) of $J/\psi \rightarrow \gamma\eta\eta$, the BES III collaboration observed most promising candidates for glueballs or multiquark structures below 2.5 GeV [14–16]. In the $\pi^- P \rightarrow \eta\pi^0\eta$ channel, the GAMS group at CERN reported a state near 1400 MeV [17,18]. The BNLE-852 collaboration reported another state, near 1600 MeV

in the $\pi^- p$ reaction, having a promising hybrid structure [18–21].

Meson spectroscopy, mainly light meson spectroscopy, gives information of the non-perturbative regime of QCD. The basic difficulty to study the light meson spectrum is that mostly resonances do not come out as narrow, isolated peaks [6,7]. Moreover, their large decay widths make them difficult to identify experimentally as well as to differentiate them as threshold or as interference effects, rather than pure resonances. Especially for scalar mesons, they are very difficult to identify due to large decay widths, and overlaps between resonances and background. Even the scalar mesons have the same quantum numbers as the vacuum. Thus, the understanding of the properties of scalar mesons may help us to understand the mechanism of symmetry breaking [6–8]. Various mesons in the low-lying sector like $f_0(980)$, $a_0(980)$, $f_0(1500)$ etc. were observed experimentally, but their specific structure and properties are not understood theoretically, nor experimentally. For example, the structure of the scalar states $f_0(1500)$ and $f_0(1710)$ have been debated since a long time [22–34]. The authors in [22–24] indicated them as mixed or rather pure glue states, respectively. References [26–32] indicated $f_0(1710)$ as a vector–vector molecular candidate and $f_0(1500)$ as a glueball. The status of these scalar states is still an open question. The study of these exotic states may give the answer to the basic questions of hadron masses, quark confinement, relevant degrees of freedom and interaction between the constituents of the same [6–8] (Table 1).

In the present study, we have investigated the molecular structures in the light flavour meson regime. Our dimesonic system consists of a meson and an antimeson ($q\bar{q} - \bar{q}q$). The masses of these states would be less than the sum of the masses of two constituent mesons [35–37]. These loosely bound dimesonic system are similar to the deuteron like (proton–neutron) bound state system. This approximation had been taken previously in Refs. [36,37] and introduced as

[a] e-mail: raiajayk@gmail.com

**Table 1** Experimentally observed states (in MeV) [1]

| States | Mass (MeV) | Width (MeV) | Possible $I^G(J^{PC})$ | Compared dimesonic states |
|---|---|---|---|---|
| $f_0(980)$ | $990 \pm 20$ | $40 - 100$ | $0^+(0^{++})$ | $K - \bar{K}$ |
| $b_1(1235)$ | $1229 \pm 03$ | $142 \pm 09$ | $1^+(1^{+-})$ | $\eta - \bar{\rho}$ |
| $h_1(1380)$ | $1386 \pm 19$ | $91 \pm 30$ | $0^-(1^{+-})$ | $K - \bar{K}^*$ |
| $a_0(1450)$ | $1474 \pm 19$ | $265 \pm 13$ | $1^-(0^{++})$ | $\rho - \bar{\omega}$ |
| $f_0(1500)$ | $1505 \pm 06$ | $109 \pm 07$ | $0^+(0^{++})$ | $\rho - \bar{\rho}$ |
| $f_2'(1525)$ | $1525 \pm 05$ | $76 \pm 10$ | $0^+(2^{++})$ | $\rho - \bar{\rho}$ |
| $f_2(1565)$ | $1562 \pm 13$ | $134 \pm 08$ | $0^+(2^{++})$ | $\omega - \bar{\omega}$ |
| $h_1(1595)$ | $1594 \pm 15$ | $384 \pm 60$ | $0^-(1^{+-})$ | $\eta' - \bar{\omega}$ |
| $a_2(1700)$ | $1722 \pm 16$ | $194 \pm 40$ | $1^-(2^{++})$ | $K^* - \bar{K}^*$ |
| $f_0(1710)$ | $1722^{+06}_{-05}$ | $135 \pm 07$ | $0^+(0^{++})$ | $K^* - \bar{K}^*$ |
| $f_2(1810)$ | $1815 \pm 12$ | $197 \pm 22$ | $0^+(2^{++})$ | $\phi - \bar{\omega}$ |

'deusons'. Furthermore, the molecular like picture has been studied by Silvestre et al. [38,39] as diquonia.

The multiquark states were predicted and studied previously in the MIT Bag model and in nonrelativistic potential models [9–13]. The molecular-like structures have been studied and proposed in various models, like potential models [35–46], the chiral SU(3) quark model approach [47], the gauge invariant model [48], the Bethe–Salpeter equation approach [49], QCD sum rules [50], the effective field theory approach [51] and the non-perturbative chiral approach [52–55]. We are using the potential model to predict the masses, digamma decays and decay widths of dimesonic systems in a variational scheme. The potential model study is successfully used to explain the heavy flavour sector of mesons as well as multiquark description of meson–antimeson or tetraquark states. The potential models are used to calculate the masses [9–13,36–42] and decay properties of various multiquark states. Recently, the potential model has been employed successfully to study various spectroscopic features of mesons [56–63]. Various authors have successfully used the nonrelativistic potential model for the study of the molecular or tetraquark structure [42,44,64–67].

In our model for the study of dimesonic states, we use the Hellmann potential with One Pion Exchange Potential (OPEP). The Hellmann potential is a superposition of the Coulomb and the Yukawa potential. The superposed potential of Coulomb and Yukawa was studied by Hellmann a long time ago [68–72]. There are several authors who applied this potential for the calculation of the bound state systems for different values of their strength parameters [73–77]. All the phenomenological potential model approaches used by the authors to study the mesons or multiquark spectra have dealt with complex interactions like, coulombic, confinement, instanton induced interaction, color, flavour and spin

dependency to accomplish a description of the bound state properties. At very short distances, the bound state system is produced due to a delicate attractive and repulsive interaction. The Hellmann potential simply accomplishes the complicated theoretical calculation for the cancellation of the attractive and repulsive interaction at short distances, causing the small binding energy of the bound state. The Hellmann potential with the OPEP used in the present model takes care of the short and the long range behaviour of the interactions. As we are aware that mesons are color neutral, we have not introduced the confinement potential for the dimesonic systems. It is well studied that the OPEP is mainly responsible for the long range part of the strong nuclear force. The concept of meson exchange interaction has been used since a long time ago for the N–N interaction [78,79] as well as for hadronic molecules [36,37,80–82].

To test the potential and mechanism employed, we first apply it to study the state $f_0(980)$, which was found in the literature to be interpreted as a molecular state [11–13,44]. Moreover, the molecular like picture has been supported by lattice QCD [83,84]. We calculate the spectra of $f_0(980)$ and obtained its mass, binding energy and root mean square radius. The results show fairly good agreement with the experimental results. Thus we are convinced and apply the same methodology to other dimesonic molecular states.

The study of the light meson sector needs a relativistic treatment. We are incorporating a relativistic correction to the kinetic energy term as well as to the meson–antimeson potential. The hydrogen like trial wave function is being used for this study. We have calculated the digamma decay width and decay width of the dimesonic systems. The study of the digamma decay of scalars helps to distinguish among different scenarios for the scalar meson structure [43]. The digamma decays of the dimesonic systems are calculated using the wave function at the origin [43]. For the decay calculation, we adopt the same formulation as used by Ref. [44], which was used to study the molecular picture of $1^{-+}$ exotic states.

The article is organised as follows. After a brief introduction, we present the theoretical framework for the study of dimesonic molecular states in semirelativistic approach with the Hellmann potential and OPE potential in Sect. 2. The calculation of digamma decays and decay widths are discussed in Sect. 3. Then we present the calculated results in Sect. 4, and the last section is dedicated to our conclusions.

## 2 Theoretical framework

In the variational approach, we have solved the Schroedinger equation by using a trial wave function. The variational parameter is obtained by using the virial theorem. The (dimesonic) molecular system is assumed to consist of

a meson–antimeson bound state. The Hamiltonian of the dimesonic system is given by [85–88]

$$H = \sqrt{P^2 + m_a^2} + \sqrt{P^2 + m_b^2} + V(r) \tag{1}$$

where $m_a$ and $m_b$ are the masses of mesons, $P$ is the relative momentum of the two mesons and $V(r)$ is the molecular interaction potential of the dimesonic system. We expand the kinetic energy term of the Hamiltonian up to $\mathcal{O}(P^6)$:

$$K.E. = \frac{P^2}{2}\left(\frac{1}{m_a} + \frac{1}{m_b}\right) - \frac{P^4}{8}\left(\frac{1}{m_a^3} + \frac{1}{m_b^3}\right)$$
$$+ \frac{P^6}{16}\left(\frac{1}{m_a^5} + \frac{1}{m_b^5}\right) + \mathcal{O}(P^8). \tag{2}$$

$V(r)$ is the molecular (meson–antimeson) potential,

$$V(r) = V^{(0)}(r) + \left(\frac{1}{m_a} + \frac{1}{m_b}\right)V^{(1)}(r) + \mathcal{O}\left(\frac{1}{m^2}\right) \tag{3}$$

where

$$V^{(0)}(r) = V(r_{12}) + V_\pi. \tag{4}$$

We consider the meson–antimeson interacting through the Hellmann potential. It is a superposition of the Coulomb and Yukawa potentials of the form [68–76]

$$V(r_{12}) = -\frac{\alpha_s}{r_{12}} + B\frac{e^{-cr_{12}}}{r_{12}}. \tag{5}$$

Here $\alpha_s$ and B are the strengths of the potential, C is the screening parameter and $r_{12}$ is the relative coordinates between meson and antimeson; the strength of the Coulomb potential is used as running coupling constant. B is the Yukawa potential strength and it takes both positive and negative values. Reference [74] has carried out a detailed study for different values of B and the screening parameter C for low-lying energy eigenvalues. For our dimesonic study, we have taken B positive.

The value of the $\alpha_s$ running coupling constant is determined through the model, namely

$$\alpha_s(M^2) = \frac{4\pi}{(11 - \frac{2}{3}n_f)ln\frac{M^2 + M_B^2}{\Lambda_Q^2}} \tag{6}$$

where $M = 2m_a m_b/(m_a + m_b)$, $M_B = 1\,\text{GeV}$, $\Lambda_Q = 0.413\,\text{GeV}$, and $n_f$ is number of flavours [89].

The non-perturbative form of $V^{(1)}(r)$ is not yet known, but leading order perturbation theory yields

$$V^{(1)}(r) = -C_F C_A \alpha_s^2/4r_{12}^2, \tag{7}$$

where $C_F = 4/3$ and $C_A = 3$ are the Casimir charges of the fundamental and adjoint representation, respectively [90]. The relativistic mass correction is found to be similar to the Coulombic term of the static potential when applied to the charmonium and to be one-fourth of the Coulombic term

for bottomonium [90]. Recently we have used this correction successfully in a study of the $B_c$ meson [85,86].

The long range OPEP is used based on the assumption that the molecular like structure of the multiquark system is as deuterium, like the structure of the nucleon [35,80]. The OPEP for the NN-interaction takes the form [91,92]

$$V_{\pi(NN)} = \frac{g_8^2}{4\pi}\frac{m_\pi}{3}(\tau_i \cdot \tau_j)$$
$$\times \left[T_\pi(r)S_{12} + \left(Y_\pi(r) - \frac{4\pi}{m_\pi^3}\delta(r)\right)\sigma_i \cdot \sigma_j\right] \tag{8}$$

where $g_8$ is a pion–nucleon coupling constant. $\boldsymbol{\tau}$ and $\boldsymbol{\sigma}$ are isospin and spin factors, respectively. Here $T_\pi(r)$, $Y_\pi(r)$ and $S_{12}$ are

$$T_\pi(r) = \left(1 + \frac{3}{m_\pi r} + \frac{3}{m_\pi^2 r^2}\right)\frac{e^{-m_\pi r}}{m_\pi r} \tag{9}$$

$$Y_\pi(r) = \frac{e^{-m_\pi r}}{m_\pi r} \tag{10}$$

$$S_{12} = 3\sigma_i \cdot \hat{r}\sigma_j \cdot \hat{r}/r^2 - \sigma_i \cdot \sigma_j. \tag{11}$$

The exchange meson having its own internal structure, to accomplish the finite size effect [91,92], the usual form factor appears due to the dressing of quarks and is assumed to be proportional to the exchange meson mass [80]. We have

$$T_{\Lambda_\pi}(r) = \left(1 + \frac{3}{\Lambda_\pi r} + \frac{3}{\Lambda_\pi^2 r^2}\right)\frac{e^{-\Lambda_\pi r}}{\Lambda_\pi r}, \tag{12}$$

$$Y_{\Lambda_\pi}(r) = \frac{e^{-\Lambda_\pi r}}{\Lambda_\pi r}. \tag{13}$$

The functions $T(r)$ and $Y(r)$ with the finite size effects take the form

$$Y(r) = \frac{\Lambda_\pi^2}{\Lambda_\pi^2 - m_\pi^2}\left[Y_\pi(r) - \frac{\Lambda_\pi^3}{m_\pi^3}Y_{\Lambda_\pi}(r)\right], \tag{14}$$

$$T(r) = \frac{\Lambda_\pi^2}{\Lambda_\pi^2 - m_\pi^2}\left[T_\pi(r) - \frac{\Lambda_\pi^3}{m_\pi^3}T_{\Lambda_\pi}(r)\right]. \tag{15}$$

A more detailed derivation of the potential can be found in Refs. [91,92]. $S_{12}$ is the usual tensor operator, it plays a prominent role in the NN-interaction. The matrix element of the tensor operator for $L = 0$ vanishes [82]. If two hadrons are in an $L = 0$ (ground) state, the term with a tensor operator vanishes as in our dimesonic case. Thus, the OPEP takes the form

$$V_\pi = \frac{1}{3}\frac{g_8^2}{4\pi}\left(\frac{m_\pi^2}{4m_a m_b}\right)(\tau_i \cdot \tau_j)(\sigma_i \cdot \sigma_j)$$
$$\times \left(\frac{e^{-m_\pi r_{ij}}}{r_{ij}} - \left(\frac{\Lambda_\pi}{m_\pi}\right)^2\frac{e^{-\Lambda_\pi r_{ij}}}{r_{ij}}\right) \tag{16}$$

where $g_8 = 0.69$ is a meson pion coupling constant, $\Lambda_\pi = km_\pi$, whereas $m_a$ and $m_b$ are constituents masses, $m_\pi =$

**Table 2** Masses of mesons (in MeV) [1]

| Meson | $K^+$ | $K^0$ | $\eta$ | $\eta'$ | $\rho$ | $\omega$ | $K^*$ | $\phi$ |
|-------|-------|-------|--------|---------|--------|----------|-------|--------|
| Mass | 493.6 | 497.6 | 547.8 | 957.7 | 775.4 | 782.6 | 895.9 | 1019.4 |

0.134 GeV and $k = 2.2$. For PV states the values of the spin–isospin factor have been taken as $(\tau_i \cdot \tau_j)(\sigma_i \cdot \sigma_j) = -3, 1$ for $I = 0, 1$. For VV states the values are taken as $(\tau_i \cdot \tau_j)(\sigma_i \cdot \sigma_j) = -6, -3, 3$ for isospin $I = 0$ and spin $S = 0, 1, 2$, respectively; whereas for isospin $I = 1$ and spin $S = 0, 1, 2$ it takes the values $(\tau_i \cdot \tau_j)(\sigma_i \cdot \sigma_j) = 2, 1, -1$. The values of the spin–isospin factor are from Refs. [36,37] and the other parameters used in pion exchange potential are from Refs. [80–82].

For the hyperfine splitting, the spin dependent interaction potential is added perturbatively and takes the form

$$V_{SD} = \frac{8}{9} \frac{\alpha_s}{m_a m_b} \mathbf{S_1} \cdot \mathbf{S_2} |\psi(0)|^2 . \tag{17}$$

The spin factor $\mathbf{S_1} \cdot \mathbf{S_2}$ can be found by the general formula $\mathbf{S_1} \cdot \mathbf{S_2} = \frac{1}{2}[(\mathbf{S_1} + \mathbf{S_2})^2 - \mathbf{S_1}^2 - \mathbf{S_2}^2]$ [40,41]
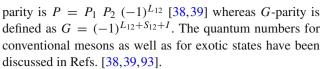
We have used the hydrogen like trial wave function

$$R_{nl}(r) = \left( \frac{\mu^3 (n-l-1)!}{2n(n+l)^3!} \right)^{\frac{1}{2}} (\mu r)^l e^{\frac{-\mu r}{2}} L_{n-l-1}^{2l+1}(\mu r), \tag{18}$$

where $\mu$ is the variational parameter and $L_{n-l-1}^{2l+1}(\mu r_{12})$ is the Laguerre polynomial. The ground state mass of the low-lying dimesonic states is calculated by obtaining the expectation value of the Hamiltonian and the variational parameter($\mu$) is obtained for each state by using the virial theorem [85–88]. We have

$$H\psi = E\psi \quad \text{and} \quad \langle \text{K.E.} \rangle = \frac{1}{2} \left\langle \frac{r \, dV(r)}{dr} \right\rangle . \tag{19}$$

We have included the kinetic energy term up to $P^6$ and the potential with correction [Eq. (3)] for the determination of $\mu$. We fix the color screening parameter $C = 0.35$ GeV for all combinations and $B = 0.4$ for the PP and PV states and $B = 1.2$ for the VV states, while the strength of the Coulomb potential $\alpha(M^2)$ is calculated as per Eq. (6). The experimental (PDG) masses of the mesons are used for the present study, as tabulated in Table 2 [1].

The angular momentum, parity, spin and isospin all are conserved in the strong interaction, being good quantum numbers for the dimesonic system. The orbital angular momentum of meson and antimeson are $L_1$ and $L_2$, respectively. In same way spin denote by $S_1$, $S_2$ and isospin $I_1$, $I_2$. Employing the coupling rules, one has the relative orbital momentum and total spin of system $L_{12}$ and $S_{12}$ whereas the total angular momentum is $\mathbf{J} = \mathbf{L_{12}} + \mathbf{S_{12}}$; $\mathbf{I} = \mathbf{I_1} + \mathbf{I_2}$. The charge conjugation of the two particle system (meson–antimeson) is given by $C = (-1)^{L_{12}+S_{12}}$ [93] while the

parity is $P = P_1 P_2 (-1)^{L_{12}}$ [38,39] whereas $G$-parity is defined as $G = (-1)^{L_{12}+S_{12}+I}$. The quantum numbers for conventional mesons as well as for exotic states have been discussed in Refs. [38,39,93].

The OPEP for the dimesonic system in Eq. (8) is spin–isospin dependent. Törnqvist in [36,37] has discussed the spin–isospin dependency of OPEP for deusons. The spin–isospin factor gives influence to the potential and decides whether a channel becomes attractive or repulsive. For VV states we got a repulsive channel for $(S, I) = (0, 1)(1, 1)(2, 0)$, while an attractive channel was found for $(S, I) = (0, 0)(1, 0)(2, 1)$. In the case of PV states the channel becomes attractive for $(S, I) = (1, 0)$, while it becomes repulsive for $(S, I) = (1, 1)$. Due to parity violation, the two pseudoscalars could not be bound by a pseudoscalar [35–37]. Thus, we could not consider OPEP for PP states. For such PP states, the Hellmann potential given in Eq. (5) is being used with a relativistic correction. The calculated masses are close to experimental measurements (PDG), tabulated in Table 3.

We have used a pseudoscalar and a vector meson for the dimesonic system, having the possible combinations (i) pseudoscalar–pseudoscalar (PP state), (ii) pseudoscalar–vector (PV state), (iii) vector–vector (VV state).

## 3 Digamma width and decay width

The digamma decay of the dimesonic molecules are estimated, using the wave function at the origin, in analogy to the two photon decay of parapositronium [43]. The digamma width for all mass combinations is given by

$$\Gamma_{\gamma\gamma} = 2\xi^2 \frac{\pi\alpha^2}{m_a m_b} |\psi(0)|^2 ; \tag{20}$$

$\alpha = e^2/4\pi$ indicates the fine-structure constant, we have the factor $\xi = \frac{1}{\sqrt{2}}$ and $m_a$ and $m_b$ are the masses of the constituent mesons.

The decay width is calculated using the wave function at the origin. The dimesonic molecular state (constituent mesons $a$ and $b$) decays into mesons $c$ and $d$. In the decay through meson exchange, the amplitude is proportional to the wave function squared at the origin [44]. The formula of $|\psi(0)|^2$ given by [44,94–96] is

$$|\psi(0)|^2 = 2M \langle \psi \mid dV/dr \mid \psi \rangle, \tag{21}$$

with $M$ the reduced mass of the system, $\psi(0)$ includes the effects of all ranges in $r$.

The decay width is

$$\Gamma = \frac{|\psi(0)|^2 l}{16\pi m_m^3} |\mathcal{M}|^2 , \tag{22}$$

**Table 3** Mass spectra, binding energy, root mean square radius and digamma decay width of dimesonic ($q\bar{q} - \bar{q}q$) systems with their $J^{PC}$ values

| System | $I^G(J^{PC})$ | $\mu$ (GeV) | $R(0)$ (GeV$^{\frac{3}{2}}$) | $\sqrt{<r^2>}$ (fm) | B.E. (MeV) | Mass (GeV) | Expt. [1] (GeV) | $\Gamma_{\gamma\gamma}$ KeV | Exp. [1] KeV | State |
|---|---|---|---|---|---|---|---|---|---|---|
| *PP states* | | | | | | | | | | |
| $K - \overline{K}$ | $0^+ (0^{++})$ | 0.219 | 0.072 | 11.63 | $-20.87$ | 0.974 | $0.990 \pm 0.020$ | 0.285 | $0.29^{+0.07}_{-0.06}$ | $f_0(980)$ |
| $\eta - \bar{\eta}$ | $0^+ (0^{++})$ | 0.265 | 0.096 | 09.63 | $-26.24$ | 1.069 | | 0.414 | | |
| $\eta - \bar{\eta}'$ | $0^+ (0^{++})$ | 0.409 | 0.185 | 06.24 | $-46.75$ | 1.458 | | 1.526 | | |
| $\eta' - \bar{\eta}'$ | $0^+ (0^{++})$ | 0.628 | 0.352 | 04.06 | $-85.22$ | 1.830 | | 1.803 | | |
| *PV states* | | | | | | | | | | |
| $\eta - \bar{\rho}$ | $1^+ (1^{+-})$ | 0.210 | 0.068 | 12.12 | $-63.82$ | 1.259 | $1.229 \pm 0.003$ | 0.208 | | $b_1(1235)$ |
| $\eta - \bar{\omega}$ | $0^- (1^{+-})$ | 0.209 | 0.067 | 12.20 | $-63.22$ | 1.267 | | 0.203 | | |
| $K - \overline{K}^*$ | $0^- (1^{+-})$ | 0.206 | 0.066 | 12.36 | $-62.60$ | 1.330 | $1.386 \pm 0.019$ | 0.237 | | $h_1(1380)$ |
| $K - \overline{K}^*$ | $1^+ (1^{+-})$ | 0.209 | 0.067 | 12.19 | $-63.51$ | 1.330 | | 0.247 | | |
| $\eta - \bar{\phi}$ | $0^- (1^{+-})$ | 0.253 | 0.090 | 10.08 | $-73.50$ | 1.493 | | 0.361 | | |
| $\eta' - \bar{\rho}$ | $1^+ (1^{+-})$ | 0.351 | 0.147 | 07.26 | $-94.25$ | 1.639 | | 0.316 | | |
| $\eta' - \bar{\omega}$ | $0^- (1^{+-})$ | 0.350 | 0.146 | 07.30 | $-93.45$ | 1.646 | $1.594 \pm 0.015$ | 0.312 | | $h_1(1595)$ |
| $\eta' - \bar{\phi}$ | $0^- (1^{+-})$ | 0.429 | 0.198 | 05.95 | $-107.4$ | 1.869 | | 0.574 | | |
| *VV states* | | | | | | | | | | |
| $\rho - \bar{\rho}$ | $0^+ (0^{++})$ | 0.192 | 0.059 | 13.27 | $-55.39$ | 1.489 | $1.505 \pm 0.006$ | 0.079 | | $f_0(1500)$ |
| $\rho - \bar{\rho}$ | $0^- (1^{+-})$ | 0.197 | 0.062 | 12.92 | $-55.00$ | 1.492 | | 0.085 | | |
| $\rho - \bar{\rho}$ | $0^+ (2^{++})$ | 0.194 | 0.060 | 13.15 | $-54.10$ | 1.500 | $1.525 \pm 0.005$ | 0.081 | $0.081 \pm 0.009$ | $f_2'(1525)$ |
| $\rho - \bar{\rho}$ | $1^- (0^{++})$ | 0.194 | 0.060 | 13.11 | $-54.25$ | 1.490 | | 0.082 | | |
| $\rho - \bar{\rho}$ | $1^+ (1^{+-})$ | 0.195 | 0.061 | 13.07 | $-54.40$ | 1.493 | | 0.082 | | |
| $\rho - \bar{\rho}$ | $1^- (2^{++})$ | 0.196 | 0.061 | 13.00 | $-54.70$ | 1.499 | | 0.084 | | |
| $\omega - \bar{\omega}$ | $0^+ (0^{++})$ | 0.201 | 0.064 | 12.67 | $-55.77$ | 1.502 | | 0.089 | | |
| $\omega - \bar{\omega}$ | $0^- (1^{+-})$ | 0.199 | 0.063 | 12.79 | $-55.31$ | 1.506 | | 0.086 | | |
| $\omega - \bar{\omega}$ | $0^+ (2^{++})$ | 0.196 | 0.061 | 13.01 | $-54.40$ | 1.514 | $1.562 \pm 0.013$ | 0.082 | $0.70 \pm 0.14$ | $f_2(1565)$ |
| $K^* - \overline{K}^*$ | $0^+ (0^{++})$ | 0.231 | 0.078 | 11.05 | $-59.34$ | 1.724 | $1.722^{+0.006}_{-0.005}$ | 0.102 | | $f_0(1710)$ |
| $K^* - \overline{K}^*$ | $0^- (1^{+-})$ | 0.229 | 0.077 | 11.14 | $-58.89$ | 1.729 | | 0.100 | | |
| $K^* - \overline{K}^*$ | $0^+ (2^{++})$ | 0.225 | 0.075 | 11.32 | $-58.01$ | 1.730 | | 0.095 | | |
| $K^* - \overline{K}^*$ | $1^- (0^{++})$ | 0.226 | 0.076 | 11.29 | $-58.16$ | 1.726 | | 0.096 | | |
| $K^* - \overline{K}^*$ | $1^+ (1^{+-})$ | 0.226 | 0.076 | 11.26 | $-58.31$ | 1.730 | | 0.096 | | |
| $K^* - \overline{K}^*$ | $1^- (2^{++})$ | 0.228 | 0.077 | 11.20 | $-58.60$ | 1.736 | $1.722 \pm 0.016$ | 0.098 | $0.30 \pm 0.05$ | $a_2(1700)$ |
| $\phi - \bar{\phi}$ | $0^+ (0^{++})$ | 0.255 | 0.091 | 10.00 | $-60.91$ | 1.970 | | 0.106 | | |
| $\phi - \bar{\phi}$ | $0^- (1^{+-})$ | 0.253 | 0.090 | 10.07 | $-60.49$ | 1.974 | | 0.104 | | |
| $\phi - \bar{\phi}$ | $0^+ (2^{++})$ | 0.250 | 0.088 | 10.22 | $-59.68$ | 1.982 | | 0.100 | | |
| $\rho - \bar{\omega}$ | $1^- (0^{++})$ | 0.196 | 0.061 | 13.04 | $-54.40$ | 1.497 | $1.474 \pm 0.019$ | 0.081 | | $a_0(1450)$ |
| $\rho - \bar{\omega}$ | $1^+ (1^{+-})$ | 0.196 | 0.061 | 13.00 | $-54.55$ | 1.500 | | 0.082 | | |
| $\rho - \bar{\omega}$ | $1^- (2^{++})$ | 0.197 | 0.062 | 12.93 | $-54.85$ | 1.506 | | 0.084 | | |
| $\phi - \bar{\rho}$ | $1^- (0^{++})$ | 0.222 | 0.074 | 11.47 | $-57.82$ | 1.730 | | 0.070 | | |
| $\phi - \bar{\rho}$ | $1^+ (1^{+-})$ | 0.223 | 0.074 | 11.44 | $-57.96$ | 1.733 | | 0.071 | | |
| $\phi - \bar{\rho}$ | $1^- (2^{++})$ | 0.224 | 0.075 | 11.38 | $-58.25$ | 1.740 | | 0.072 | | |
| $\phi - \bar{\omega}$ | $0^+ (0^{++})$ | 0.228 | 0.077 | 11.17 | $-59.10$ | 1.735 | | 0.076 | | |
| $\phi - \bar{\omega}$ | $0^- (1^{+-})$ | 0.226 | 0.076 | 11.26 | $-58.65$ | 1.739 | | 0.074 | | |
| $\phi - \bar{\omega}$ | $0^+ (2^{++})$ | 0.223 | 0.074 | 11.44 | $-57.79$ | 1.747 | $1.815 \pm 0.012$ | 0.071 | | $f_2(1810)$ |

where $m_m$ is the mass of a dimesonic molecule and $l$ is the magnitude of the 3-momentum of the decay product, given by

$$l^2 = \frac{(m_m^4 + m_c^4 + m_d^4)}{4m_m^4} - \frac{(m_m^2 m_c^2 + m_m^2 m_d^2 + m_c^2 m_d^2)}{2m_m^4}. \tag{23}$$

$m_a$ and $m_b$ are the masses of the constituent mesons and $m_c$ and $m_d$ are the masses of the product mesons. $\mathcal{M}$ is the amplitude,

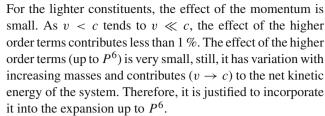$$\mathcal{M} = \frac{\alpha_s^2}{q^2 - m_q^2} \left( \frac{\Lambda^2 - m_q^2}{\Lambda^2 - q^2} \right). \tag{24}$$

$m_q$ and q are the mass and 3-momentum of the exchange mesons (for present work, we consider only a pion). $\Lambda$ is the free parameter which takes care of the off-shell effects at the vertices because of the internal structure of the mesons. The digamma decay widths are tabulated in Table 3 along with the masses. The decay width of the compared states as well as our predicated states are tabulated in Table 4.

## 4 Results and discussion

By using the Hellmann potential, the OPE potential and a relativistic correction, we have solved the Schroedinger equation to extract the masses, binding energy, decay widths and digamma decay widths for dimesonic states. In various combination of dimesonic states, like the PP, PV and VV states, we have calculated the possible molecular like structure in the light flavoured sector. Our calculated results are tabulated in Tables 3 and 4.

To describe the molecular picture of dimesonic states, we have incorporated the short range and long range behaviour of the potential. As the constituent of the molecule (meson) itself is color neutral and comes with a small binding energy and large radius ($r$ in $fm$) in comparison to the constituent size, we do not need to introduce the confinement potential and so we have not dealt with the fundamental quark gluon condense state in the present study. Thus, we have not incorporated any mixing scheme of gluonia and quarkonia. Still, the results obtained in the present study have reasonably good agreement with experimental measurements and explain the molecular picture well.

We have expanded the kinetic energy term up to $\mathcal{O}(P^6)$. In the series expansion of the kinetic energy, For $v \ll c$, the effect of the higher order term of the momentum $P^{2n}$ ($n > 2$) is negligible, even more, the higher order term has poor convergence. While the expansion term up to $P^4$ does not have a lower bound. So, the usable expansion to incorporate the relativistic effect is being up to $P^6$ [91,92]. We have dealt with the systems which have constituent masses below 2 GeV.

For the lighter constituents, the effect of the momentum is small. As $v < c$ tends to $v \ll c$, the effect of the higher order terms contributes less than 1 %. The effect of the higher order terms (up to $P^6$) is very small, still, it has variation with increasing masses and contributes ($v \to c$) to the net kinetic energy of the system. Therefore, it is justified to incorporate it into the expansion up to $P^6$.

The correction used in the potential has its dominant effect on the potential energy. In our calculation, the effect of the correction to the potential energy part is increasing as mass of the system decreasing, and, it is about to be 25–40 %. The effect of correction to potential is approximately 38 % in the lightest dimesonic system ($K - \overline{K}$) of this work, while the heaviest system $\phi - \overline{\phi}$ has a contribution of about 28 %. We have calculated the partial decay width as per Eq. (22). The parameter $\Lambda$ is assumed to be proportional to the mass of the dimesonic state, $\Lambda = \mathcal{K} m_m$. We have chosen the Yukawa strength parameter and the color screening parameter $B = 0.4$ and $C = 0.35$, respectively, to find the mass spectra for the $K - \overline{K}$ molecule, which is believed to be $f_0(980)$. For the decay calculation of $K - \overline{K}$, we took $\mathcal{K} = 1.262$. Our calculated results for mass, digamma and decay width are close to the PDG values [1]. Thus, we fixed these parameters for the calculation of all PP and PV states, while for the VV state we took $B = 1.2$. For the dimesonic states having masses between 1 to 1.6 GeV, the constant $\mathcal{K} = 1.085$, whereas for the states between 1.6 to 2 GeV, $\mathcal{K} = 0.931$. In the PP states, we used the Hellmann potential with a relativistic correction. Due to parity violation, the OPEP cannot be applied to the calculation of the PP states. We have

$$m_{m\,f_0(980)} = 0.974 \,\text{GeV}; \quad \Gamma_{\gamma\gamma} = 0.28 \,\text{KeV};$$
$$\Gamma_{(f_0(980))} = 94 \,\text{MeV}.$$

Our results for $f_0(980)_{k\overline{K}}$ are in good agreement with the suggested mass and decay width ($0.982 \pm 0.003$ and $80 \pm 10$ MeV) of Ref. [97]. The calculated digamma width of $f_0(980)$ is in close agreement with other theoretical predictions [48,97–101]. The $\pi\pi$ decay mode of $f_0(980)$ is dominant and also agrees with Ref. [1]. For the molecular state, one should have a small binding energy and a large radius (compared to the constituent energy and radius). Our results satisfied these conditions. The mass and decay properties are close to the experimental measurements. Thus, we employ the same methodology to calculate the properties of all the meson–antimeson combinations. The computed results are tabulated in Tables 3 and 4.

Pseudoscalar–vector (PV) states

In the PV states, the $\pi V$ system is the lightest dimesonic state possible. In the present work, we have not considered $\pi V$ systems. The pion is too light as a constituent for dimesonic

**Table 4** Decay width of dimesonic (molecular) states(in MeV). The decay width is calculated for experimentally seen decay modes listed in PDG [1]. The other dimesonic states are also tabulated with isospin–spin $(I, S)$

| States | Dimesonic decay widths (in MeV) | | | Total width | PDG [1] | Others | Current status in PDG [1] |
|---|---|---|---|---|---|---|---|
| | (In different decay modes) | | | | | | |
| $f_0(980)_{(k\bar{k})}$ | $(49)_{\pi\pi}$ | $(33)_{\pi\eta}$ | $(12)_{\pi\omega}$ | 94 | 50–100 | $91^{+30}_{-20}$ [118] $108$ [44] | OK |
| $b_1(1235)_{(\eta\bar{\rho})}$ | $(89)_{\pi\omega}$ | $(43)_{\pi\phi}$ | – | 132 | $142 \pm 9$ | $151 \pm 31$ [119] $113 \pm 12$ [120] | OK |
| $h_1(1380)_{(k\bar{k}*)}$ | $(109)_{\pi\pi}$ | $(71)_{\pi\eta}$ | $(88)_{\pi\omega}$ | 268 | $91 \pm 30$ | $170 \pm 80$ [104–106] | NC! |
| $a_0(1450)_{(\rho\bar{\omega})}$ | $(37)_{\pi\eta}$ | $(32)_{K\bar{K}}$ | $(25)_{\pi\eta'}$ | 94 | $265 \pm 13$ | $265 \pm 30$ [121,122] $196 \pm 10$ [123] | OK |
| $f_0(1500)_{(\rho\bar{\rho})}$ | $(50)_{\pi\pi}$ | $(29)_{\eta\eta}$ | $(31)_{K\bar{K}}$ | 110 | $109 \pm 7$ | $108 \pm 33$ [102,103] $66 \pm 10$ [124] | OK |
| $f_2'(1525)_{(\rho\bar{\rho})}$ | $(25)_{K\bar{K}}$ | $(23)_{\eta\eta}$ | $(34)_{\pi\pi}$ | 82 | $76 \pm 10$ | $69 \pm 22$ [125] $75 \pm 4$ [126] | OK |
| $f_2(1565)_{(\omega\bar{\omega})}$ | $(33)_{\pi\pi}$ | $(25)_{K\bar{K}}$ | $(23)_{\eta\eta}$ | 81 | $134 \pm 8$ | $113 \pm 23$ [121,122] $119 \pm 24$ [102,103] | NC! |
| $h_1(1595)_{(\eta'\bar{\omega})}$ | $(63)_{\omega\eta}$ | – | – | 63 | $384 \pm 60$ | $384 \pm 60$ [127] | NC! |
| $a_2(1700)_{(k*\bar{k}*)}$ | $(75)_{\pi\eta}$ | $(69)_{K\bar{K}}$ | $(37)_{\rho\omega}$ | 181 | $194 \pm 40$ | $151 \pm 22$ [128] $187 \pm 60$ [129] | NC! |
| $f_0(1710)_{(k*\bar{k}*)}$ | $(45)_{K\bar{K}}$ | $(43)_{\eta\eta}$ | $(55)_{\pi\pi}$ | 143 | $135 \pm 7$ | $139^{+11}_{-12}$ [130–132] $145 \pm 8$ [111–114] | OK |
| $f_2(1810)_{(\phi\bar{\omega})}$ | $(75)_{\pi\pi}$ | $(62)_{\eta\eta}$ | $(59)_{K\bar{K}}$ | 196 | $197 \pm 22$ | $228^{+21}_{-20}$ [130–132] | NC! |
| $(\eta\bar{\eta})_{(0,0)}$ | $(756)_{\pi\pi}$ | $(554)_{\pi\eta}$ | $(286)_{K\bar{K}}$ | 1596 | – | – | – |
| $(\eta\bar{\eta'})_{(0,0)}$ | $(477)_{\pi\pi}$ | $(411)_{\pi\eta}$ | $(355)_{K\bar{K}}$ | 1243 | – | – | – |
| $(\eta'\bar{\eta'})_{(0,0)}$ | $(841)_{\pi\pi}$ | $(769)_{\pi\eta}$ | $(714)_{K\bar{K}}$ | 2324 | – | – | – |
| $(\eta\bar{\omega})_{(0,1)}$ | $(114)_{\pi\omega}$ | $(89)_{\pi\eta}$ | $(85)_{\pi\rho}$ | 288 | – | – | – |
| $(K\bar{K}*)_{(1,1)}$ | $(74)_{\pi\omega}$ | $(77)_{\pi\rho}$ | $(74)_{K\bar{K}}$ | 225 | – | – | – |
| $(\eta\bar{\phi})_{(0,1)}$ | $(70)_{\pi\omega}$ | $(44)_{\eta\omega}$ | $(70)_{\pi\rho}$ | 184 | – | – | – |
| $(\eta'\bar{\rho})_{(1,1)}$ | $(87)_{\pi\omega}$ | $(87)_{\pi\rho}$ | $(58)_{KK*}$ | 232 | – | – | – |
| $(\eta'\bar{\phi})_{(0,1)}$ | $(175)_{\pi\omega}$ | $(176)_{\pi\rho}$ | $(139)_{KK*}$ | 490 | – | – | – |
| $(\rho\bar{\rho})_{(0,1)}$ | $(30)_{\pi\rho}$ | $(30)_{\pi\omega}$ | $(15)_{KK*}$ | 75 | – | – | – |
| $(\rho\bar{\rho})_{(1,0)}$ | $(31)_{\pi\rho}$ | $(15)_{KK*}$ | $(31)_{\pi\omega}$ | 77 | – | – | – |
| $(\rho\bar{\rho})_{(1,1)}$ | $(29)_{\pi\rho}$ | $(29)_{\pi\omega}$ | $(14)_{KK*}$ | 72 | – | – | – |
| $(\rho\bar{\rho})_{(1,2)}$ | $(35)_{\pi\pi}$ | $(26)_{K\bar{K}}$ | $(25)_{\pi\omega}$ | 86 | – | – | – |
| $(\omega\bar{\omega})_{(0,0)}$ | $(46)_{\pi\pi}$ | $(35)_{K\bar{K}}$ | $(33)_{\pi\omega}$ | 114 | – | – | – |
| $(\omega\bar{\omega})_{(0,1)}$ | $(30)_{\pi\rho}$ | $(15)_{KK*}$ | $(29)_{\pi\omega}$ | 74 | – | – | – |
| $(K*\bar{K}*)_{(0,1)}$ | $(50)_{\pi\omega}$ | $(40)_{\eta\omega}$ | $(36)_{KK*}$ | 126 | – | – | – |
| $(K*\bar{K}*)_{(0,2)}$ | $(60)_{\pi\pi}$ | $(49)_{K\bar{K}}$ | $(47)_{\pi\omega}$ | 156 | – | – | – |
| $(K*\bar{K}*)_{(1,0)}$ | $(52)_{\pi\pi}$ | $(43)_{K\bar{K}}$ | $(42)_{\pi\omega}$ | 137 | – | – | – |
| $(K*\bar{K}*)_{(1,1)}$ | $(48)_{\pi\omega}$ | $(48)_{\pi\rho}$ | $(35)_{KK*}$ | 131 | – | – | – |
| $(\phi\bar{\phi})_{(0,0)}$ | $(21)_{\pi\pi}$ | $(18)_{K\bar{K}}$ | $(9)_{K*K*}$ | 48 | – | – | – |
| $(\phi\bar{\phi})_{(0,1)}$ | $(19)_{\pi\omega}$ | $(20)_{\pi\rho}$ | $(16)_{KK*}$ | 55 | – | – | – |
| $(\phi\bar{\phi})_{(0,2)}$ | $(28)_{\pi\pi}$ | $(25)_{K\bar{K}}$ | $(24)_{\pi\omega}$ | 77 | – | – | – |
| $(\rho\bar{\omega})_{(1,1)}$ | $(29)_{\pi\omega}$ | $(40)_{\pi\pi}$ | $(14)_{KK*}$ | 83 | – | – | – |

**Table 4** continued

| States | Dimesonic decay widths (in MeV) | | | Total width | PDG [1] | Others | Current status in PDG [1] |
|---|---|---|---|---|---|---|---|
| | (In different decay modes) | | | | | | |
| $(\rho\overline{\omega})_{(1,2)}$ | $(34)_{\pi\pi}$ | $(26)_{K\overline{K}}$ | $(25)_{\pi\omega}$ | 85 | – | – | – |
| $(\phi\overline{\rho})_{(1,0)}$ | $(51)_{\pi\pi}$ | $(42)_{K\overline{K}}$ | $(41)_{\pi\omega}$ | 134 | – | – | – |
| $(\phi\overline{\rho})_{(1,1)}$ | $(47)_{\pi\omega}$ | $(47)_{\pi\rho}$ | $(35)_{KK^*}$ | 129 | – | – | – |
| $(\phi\overline{\rho})_{(1,2)}$ | $(81)_{\pi\pi}$ | $(67)_{K\overline{K}}$ | $(64)_{\pi\omega}$ | 212 | – | – | – |
| $(\phi\overline{\omega})_{(0,0)}$ | $(53)_{\pi\pi}$ | $(44)_{K\overline{K}}$ | $(42)_{\pi\omega}$ | 139 | – | – | – |
| $(\phi\overline{\omega})_{(0,1)}$ | $(39)_{\pi\phi}$ | $(35)_{KK^*}$ | $(47)_{\pi\omega}$ | 121 | – | – | – |

*NC!* not confirmed

states, which interact through exchange of pion itself. The pion as a constituent, carries a large kinetic energy and it is difficult to overcome by potential energy to bound a molecule [36,37]. With the reasonably close mass spectra and quantum numbers, we have found the three states $b_1(1235)$, $h_1(1380)$ and $h_1(1595)$, which could be compared with the $\eta - \overline{\rho}$, $K - \overline{K}^*$, $\eta' - \overline{\omega}$ dimesonic states, respectively. The mass of $b_1(1235)_{(\eta\overline{\rho})}$ is fairly close to experimental observation. We have

$$m_{mb_1(1235)} = 1.259 \text{ GeV}; \quad \Gamma_{\gamma\gamma} = 0.20 \text{ KeV};$$
$$\Gamma_{(b_1(1235))} = 132 \text{ MeV}.$$

$\pi\omega$ is an experimentally observed dominant decay mode and our results are in good agreement. We have

For $h_1(1380)$
$$m_{mh_1(1380)} = 1.330 \text{ GeV}; \quad \Gamma_{\gamma\gamma} = 0.23 \text{ KeV};$$
$$\Gamma_{(h_1(1380))} = 268 \text{ MeV}.$$
For $h_1(1595)$
$$m_{mh_1(1595)} = 1.646 \text{ GeV}; \quad \Gamma_{\gamma\gamma} = 0.31 \text{ KeV};$$
$$\Gamma_{(h_1(1595))} = 63 \text{ MeV}.$$

In the case of $h_1(1380)_{(K\overline{K}*)}$, our calculated decay widths are overestimated. Moreover, the mass of the state is underestimated by around 50 MeV. For $f_1(1595)_{(\eta'\overline{\omega})}$, the decay width is unacceptably underestimated as regards the experimental measurement with the $\omega\eta$ observed decay mode. The mass of the state is also away from PDG values around 40 MeV. Thus, the obtained results indicate the rejection of the molecular interpretation of both states. Thus, in the PV state calculations, the $b_1(1235)$ is the only state that has been found to have a strong candidature for the dimesonic molecule.

Vector–vector (VV) states

In the VV combination, the dependency of one pion interaction potential on the spin–isospin factor gives possibilities of

the numbers of combinations for dimesonic molecular like states [36,37,82]. We have already discussed in the previous section about the matrix element that we have attractive and repulsive channels of the spin–isospin factors. We have found bound states in repulsive spin–isospin channels, showing the dominance of the Hellmann potential and the mass correction over pion exchange. This can be clearly seen from the binding energy tabulated in Table 4 for a state of the same spin with different isospin. With a different spin–isospin combination, we have compared experimentally observed states with our dimesonic molecular states, with comparable mass spectra and quantum numbers. The states $f_0(1500)$, $f'_2(1525)$, $f_2(1565)$, $a_0(1450)$, $f_0(1710)$, $a_2(1700)$ and $f_2(1810)$ compared with different vector–vector combinations are shown in Table 3.

$f_0(1500)$ is compared as a $\rho - \overline{\rho}$ molecule with $(S, I) = (0, 0)$, falling in the 1500 GeV mass regime. The computed mass and decay widths are comparable with experimental values [102,103] and with Refs. [102,103], with a suggested mass of 1.522±0.005 GeV and a decay width of 108±8 MeV. In Ref. [97] is suggested a decay width of 131 ± 15 MeV, and also in Refs. [104–108]. We have found that the $\pi\pi$ decay mode is dominant. Experimentally two photon decay has not been seen yet. We have

$$m_{m f_0(1500)} = 1.489 \text{ GeV}; \quad \Gamma_{\gamma\gamma} = 0.079 \text{ KeV};$$
$$\Gamma_{(h_1(1500))} = 110 \text{ MeV}.$$

The state $f'_2(1525)$ has been compared with the $\rho - \overline{\rho}$ dimesonic state, with $(S, I) = (2, 0)$. Our calculated decay width for $f'_2(1525)$ is consistent with Refs. [1,109] whereas the digamma width is in agreement with Refs. [1,100,110]. We have

$$m_{m f'_2(1525)} = 1.500 \text{ GeV}; \quad \Gamma_{\gamma\gamma} = 0.081 \text{ KeV};$$
$$\Gamma_{(f'_2(1525))} = 82 \text{ MeV}.$$

The state $f_2(1565)$ is compared with the $\omega - \overline{\omega}$ molecule. The calculated mass of this state is underestimated by around

40 MeV with the PDG value [1], and the calculated digamma decay width is being underestimated by about one-ninth of the recent PDG value [1]. Even more, the calculated decay width for the observed decay modes are also far away from the PDG values [1]. We have

For $f_2(1565)$
$$m_{m\,f_2(1565)} = 1.514\,\text{GeV}; \quad \Gamma_{\gamma\gamma} = 0.082\,\text{KeV};$$
$$\Gamma_{(f_2(1565))} = 81\,\text{MeV}.$$

The states $f_0(1710)$ and $a_2(1700)$ are compared with the $K^* - \overline{K}^*$ dimesonic molecule with spin states $S = 0, 2$, respectively. The mass of $f_0(1710)_{k^*\overline{K}^*}$ is in good agreement with PDG [1] and relatively close to Ref. [97] (1.750 ± 0.020 GeV) and Refs. [111–115]. Even the computed decay width is consistent with current experiment [1] and with Refs. [111–114,116]. We have

$$m_{m\,f_0(1710)} = 1.724\,\text{GeV}; \quad \Gamma_{\gamma\gamma} = 0.10\,\text{KeV};$$
$$\Gamma_{(f_0(1710))} = 143\,\text{MeV}.$$

The mass of $a_2(1700)_{k^*\overline{K}^*}$ is in excellent agreement with the experimental PDG value [1]. The digamma decay is found at one-third of the PDG value (0.30 ± 0.05 KeV) [1], but the decay width is in good agreement with the experimental values for the observed decay modes [1]. We have

$$m_{m\,a_2(1700)} = 1.736\,\text{GeV}; \quad \Gamma_{\gamma\gamma} = 0.098\,\text{KeV};$$
$$\Gamma_{(a_2(1700))} = 181\,\text{MeV}.$$

Furthermore, we compared the $\rho - \overline{\omega}$ and $\phi - \overline{\omega}$ dimesonic molecules with the states $a_0(1450)$ and $f_2(1810)$, respectively. The mass of $a_0(1450)_{\rho\overline{\omega}}$ is in agreement with the PDG value [1]. The decay width of $a_0(1450)_{\rho\overline{\omega}}$ has been found far away from the PDG value [1], enforcing us to rule it out as a dimesonic molecule. We have

$$m_{m\,a_0(1450)} = 1.497\,\text{GeV}; \quad \Gamma_{\gamma\gamma} = 0.081\,\text{KeV};$$
$$\Gamma_{(a_0(1450))} = 94\,\text{MeV}.$$

The mass of $f_2(1810)_{\phi\overline{\omega}}$ is off around 50 MeV from the experimental measurement [1], but the decay widths are fairly comparable to PDG values in the observed decay modes. We have

$$m_{m\,f_2(1810)} = 1.747\,\text{GeV}; \quad \Gamma_{\gamma\gamma} = 0.071\,\text{KeV};$$
$$\Gamma_{(f_2(1810))} = 196\,\text{MeV}.$$

Anisovich et al. [117] made a remark on the status of the state $f_2(1810)$ such that the state may be confused with $f_0(1790)$. Reference [117] has note that, if there was not any confusion between $f_2(1810)$ and $f_0(1790)$, there should be a missing $0^{++}$ state. As we observed throughout our calculated results, all states (except a few states) are underestimated by approximately 20–40 MeV. If we consider it as a limitation of our model, we can compare the state $f_0(1790)$ with

$\phi - \overline{\omega}$, with $(S, I) = (0, 0)$. So it may be possible that these two states $f_2(1810)$ and $f_0(1790)$ have the molecular structure of $\phi - \overline{\omega}$ with spin state $S = 0, 2$, respectively. But the experimental status of neither state is confirmed. Thus, it needs more attention theoretically as well experimentally. Our results favoured the molecular picture.

The status of the scalar states $f_0(1500)$ and $f_0(1710)$ as a molecule, guleball or glue mixed state have been debated since a long time ago [22–34]. The glueball and quarkonia with the same quantum number and a nearly equal mass may have interfered with each other and formed a new state. If the one bare glueball and one or more quarkonia interfere, one needs the mixing scheme to explain them. This interference or mixing of the state could be solved in a mass matrix formalism or in a linear combination of pure quarkonia and gluonia states by finding the linear coefficients, which mainly depends on the decay properties [23]. The authors of Ref. [22] have predicated $f_0(1500)$ as a glue mixture with $s\overline{s}$ component and $f_0(1710)$ as predominantly a pure glueball, as also in Refs. [23,24]. In Ref. [25] one has indicated the $f_0(1710)$ as a glueball candidate. References [26–32] have indicated $f_0(1710)$ as a vector–vector molecular candidate and $f_0(1500)$ as a glueball. So far, as per the present literature, the structure has remained unclear and debatable of the $f_0(1500)$ and $f_0(1710)$. Moreover, in the recent review of particle data [1] one has noted the status of the scalar states, in which $f_0(1710)$ together with $f_2'(1525)$ were interpreted as bound systems of two vector mesons [1,30]. The molecular picture could be tested in radiative $J/\psi$ decays as well as radiative decays of the states themselves [1,33,34]. The vector component of $f_0(1710)$ might have the origin of the enhancement seen in $J/\psi \longrightarrow \gamma\varphi\omega$ near threshold as observed at BES [1,31,32]. The scenario of these states will may become clear in future experiments like PANDA at FAIR.

Beside these, we have also calculated the decay width of the remaining dimesonic states and as listed in Table 4, these states may be identified in future experimental measurements.

## 5 Conclusion

In this paper, we are able to calculate the $S$-wave masses, digamma and decay widths of the dimesonic states in the light meson sector. Here, we would like to say that the dimesonic model becomes more accurate if the binding energy of the constituents is small compared to their masses. We compared many states which are experimentally observed and predicted theoretically and having a promising non-$q\overline{q}$ structure as the dimesonic states. The calculated results are in fairly good agreement with experimental measurements as well as theoretical predictions. On the basis of mass spectra, decay widths

and in some cases digamma widths, we are able to identify some dimesonic (meson–antimeson) states. We have calculated the decay widths for experimentally observed decay modes for each of the compared states.

In our present study, we strongly recommend the states $f_0(980), b_1(1235), f_2'(1525), f_0(1710)$ as meson–antimeson molecules. Furthermore, the states $h_1(1380)$, $a_0(1450)$, $f_2(1565)$ and $h_1(1595)$ in the calculation have been found with deviated masses and decay widths from the experimental measurements, which rules out their candidature as dimesonic molecules. Additionally, some states like $f_0(1500)$, $a_2(1700)$ and $f_2(1810)$ as regards the calculated results have a little bit of variation in the decay widths, but in some decay modes, the decay widths are fairly close to some experimental results [104–106,120,129]. Some states like $a_2(1700)$, $f_2(1810)$ and $f_0(1790)$ have an unconfirmed experimental status, needing more attention from experimentalist as well as from theoreticians.

Finally, we have predicted the masses, decay widths and digamma widths of the $S$-wave dimesonic molecular states (light sector). In the future we would like to employ this model to calculate the P-state masses and decay properties for light sector as well as for the heavy sector dimesonic systems.

### References

1. K.A. Olive et al., Chin. Phys. C **38**, 090001 (2014)
2. A. Ali, PoS BEAUTY **2011**, 002 (2011). arXiv:1108.2197 [hep-ph]
3. M. Gersabeck, Mod. Phys. Lett. A **27**, 1230026 (2012). arXiv:1207.2195 [hep-ex]
4. S.L. Olsen, Prog. Theor. Phys. Suppl. **193**, 38 (2012)
5. L. Li (BESIII Collaboration), Nucl. Phys. Proc. Suppl. 107, 225–227 (2012)
6. N. Brambilla et al., Eur. Phys. J. C **71**, 1534 (2011)
7. N. Brambilla et al. (2014). arXiv:1404.3723v2 [hep-ph]
8. Y.-L. Ma (2009). arXiv:0906.3842v2 [hep-ph]
9. R.L. Jaffe, Phys. Rev. D **38**, 195 (1977)
10. R.L. Jaffe, Phys. Rev. D **15**, 267 (1977)
11. J. Weinstein et al., Phys. Rev. D **27**, 588 (1983)
12. J. weinstein et al., Phys. Rev. D **41**, 2236 (1990)
13. J. weinstein et al., Phys. Rev. D **47**, 911 (1993)
14. M. Ablikim et al., Phys. Rev. D **87**, 092009 (2013)
15. H.-B. Li, (BESIII collaboration), EPJ Web of Conf. **72**, 00011 (2014)
16. L. Dong (2013). arXiv:1310.4409v1 [hep-ph]
17. D. Alde et al., Phys. Lett. B **205**, 397 (1988)
18. D.S. Carman, J. Phys.: Conf. Ser. **69**, 012011 (2007)
19. G.S. Adams et al., Phys. Rev. Lett. **81**, 5760 (1998)
20. E.I. Ivanov et al., Phys. Rev. Lett. **86**, 3977 (2001)
21. J. Kuhn et al., Phys. Lett. B **595**, 109 (2004)
22. S. Janowski et al., Phys. Rev. D **90**, 114005 (2014)
23. W.S. Carvalho et al., Eur. Phys. J. C **17**, 173 (2000)
24. D. Parganlija et al., Phys. Rev. D **87**, 014011 (2013)
25. F. Brünner et al., Phys. Rev. D **91**, 106002 (2015). arXiv:1504.05815 [hep-ph]
26. L.S. Geng, E. Oset, Phys. Rev. D **79**, 074009 (2009)
27. S. Choe, Soryushiron Kenkyu 95: D 87. arXiv:hep-ph/9705419v1 (1997)
28. E. Klempt, A. Zaitsev, Phys. Rep. **454**, 1 (2007)
29. A. Martnez Torres et al., Phys. Lett. B **719**, 388 (2013)
30. R. Molina et al., Phys. Rev. D **78**, 114018 (2008)
31. C. Garca-Recio et al., Phys. Rev. D **87**, 096006 (2013)
32. M. Ablikim et al., (BES Collaboration), Phys. Rev. Lett. **96**, 162002 (2009)
33. L.S. Geng et al., Eur. Phys. J. A **44**, 305 (2010)
34. T. Branz et al., Phys. Rev. D **81**, 054037 (2010)
35. C. Amsler, N.A. Törnqvist, Phys. Rep. **389**, 61 (2004)
36. N.A. Törnqvist, Phys. Rev. Lett. **67**, 557 (1991)
37. N.A. Törnqvist, Z. Phys. C **61**, 525 (1994)
38. B. Silvestre-Brac, C. Semay, Z. Phys. C **57**, 273–282 (1993)
39. B. Silvestre-Brac, C. Semay, Z. Phys. C **59**, 457–470 (1993)
40. A.K. Rai et al., Nucl. Phys. A **782**, 406 (2007)
41. A.K. Rai et al., Indian J. Phys. **80**, 387 (2006)
42. S. Patel et al., Eur. Phys. J. A **50**, 131 (2014)
43. C. Hanhart et al., Phys. Rev. D **75**, 074015 (2007)
44. R. Zhang et al., Phys. Rev. D **65**, 096005 (2002)
45. M. Iwasaki, F. Takagi, Phys. Rev. D **77**, 054020 (2008)
46. A. Bhattacharya et al., Int. J. Theor. Phys. **51**, 206 (2011)
47. Y.-R. Liu et al., Phys. Rev. C **80**, 015208 (2009)
48. T. Branz et al., Phys. Rev. D **78**, 114004 (2008)
49. X.-L. Ren et al., Eur. Phys. J. A **50**, 133 (2014)
50. J.-R. Zhang, G.-F. Chen, Phys. Rev. D **86**, 116006 (2012)
51. C. Hidalgo-Duque et al., Phys. Rev. D **87**, 076006 (2013)
52. J.A. Oller et al., Phys. Rev. D **59**, 074001 (1999)
53. J.A. Oller et al., Errata. Phys. Rev. D **60**, 099906 (1999)
54. J.A. Oller et al., Phys. Rev. D **75**, 099903 (2007)
55. J.A. Oller et al., Nucl. Phys. A **620**, 438456 (1997)
56. J.-B. Liu, M.-Z. Yang, Phys. Rev. D **91**, 094004 (2015)
57. J.-K. He et al., Int. J Mod. Phys.: Conf. Ser. **29**, 1460246 (2014)
58. K. Ablakulov, Z. Narzikulov, Phys. Atom. Nucl. **78**, 105 (2015)
59. K.B. Vijaya kumar et al., Chin. Phys. C 34, 1396 (2010)
60. K.B. Vijaya kumar et al., Indian J. Pure Appl. Phys. 52, 369 (2014)
61. K.B. Vijaya kumar et al., Indian J. Phys. 87, 493 (2013)
62. S. Patel et al. (2015). arXiv:1504.01103v1 [hep-ph]
63. L.D. Sebitla, Chiang Mai J. Sci. **34**, 165 (2006)
64. D. Janc, M. Rosina, Few-body Syst. **35**, 175 (2004)
65. J. Vijande et al., Phys. Rev. D **79**, 074010 (2009)
66. J. Vijande et al., Phys. Rev. D **79**, 037501 (2009)
67. M. Cardoso, P. Bicudo, Acta Phys. Polon. B (Proc. Suppl.) 8, 39 (2015)
68. H. Hellmann, Acta Physicochim. URSS **44**, 913 (1935)
69. H. Hellmann, Acta Physicochim. URSS **4**, 225 (1936)
70. H. Hellmann, Acta Physicochim. URSS **4**, 324 (1936)
71. H. Hellmann, J. Chem. Phys. **3**, 61 (1935)
72. H. Hellmann, W. Kassatotchkin, J. Chem. Phys. **4**, 324 (1936)
73. A.K. Roy et al., J. Math. Chem. **44**, 260 (2008)
74. J. Adamowaski, Phys. Rev. A **31**, 43 (1985)
75. M. Hamzavi et al., Commun. Theor. Phys. **60**, 1 (2013)

76. I. Nasser et al., Mol. Phys. **112**, 2608 (2014)
77. H.A. Pohl, D.R. Fowler, Int. J. Quan. Chem. **8**, 435–450 (1974)
78. R. Machleidt et al., Phys. Rep. **149**, 1–89 (1987)
79. M. Naghdi, Phys. Part. Nucl. **5**, 924 (2014)
80. S. Takeuchi, Nucl. Phys. A **790**, 502c–505c (2007)
81. M. Furuichi et al., Phys. Rev. C **68**, 034001 (2003)
82. T.E.O. Ericson et al., Phys. Lett. B **309**, 426–430 (1993)
83. M. Alford, R.L. Jaffe, Nucl. Phys. B **578**, 367 (2000)
84. C. Stewart, R. Koniuk, Phys. Rev. D **57**, 5581 (1998)
85. N. Devlani et al., Eur. Phys. J. A **48**, 104 (2012)
86. N. Devlani et al., Eur. Phys. J. A **50**, 154 (2014)
87. N. Devlani et al., Phys. Rev. D. **84**, 074030 (2011)
88. N. Devlani et. al., Int. J. Theor. Phys. **52**, 2196 (2013)
89. D. Ebert et al., Phys. Rev. D **79**, 114029 (2009)
90. Y. Koma, M. Koma, H. Wittig, Phys. Rev. Lett **97**, 122003 (2006)
91. M.W. Paris, V.R. Pandharipande, Phys. Rev. C **62**, 015201 (2000)
92. V.R. Pandharipande, S.C. Pieper, R. Schiavilla, Notes on nuclear forces on light nuclei. http://minimafisica.biodec.com/Members/k/Schiavilla-notes.
93. C.A. Meyer, Y. Van haarlem, Phys. Rev. C **82**, 025208 (2010)
94. C. Quigg, J. Rosner, Phys. Rep. **56**, 167 (1979)
95. C. Quigg, J. Rosner, Phys. Lett. B **71**, 153 (1977)
96. X.-Q. Li et al., Phys. Rev. D **55**, 1421 (1997)
97. D. Barberis et al., Phys. Lett. B **453**, 316 (1999)
98. T. Oest et al., (JADE Collaboration), Z. Phys. C **47**, 343 (1990)
99. R. Delbourgo et al., Phys. Lett. B **446**, 332 (1999)
100. T. Barnes et al., Phys. Lett. B **165**, 434 (1999)
101. S. Krewald et al., Phys. Rev. D **69**, 016003 (2004)
102. A. Bertin et al., Phys. Rev. D **57**, 55 (1998)
103. A. Bertin et al., Phys. Lett. B **408**, 476 (1997)
104. A. Abele et al., (Crystal Barrel Collaboration), Eur. Phys. J C **19**, 667 (2001)
105. A. Abele et al., Phys. Lett. B **415**, 280 (1997)
106. A. Abele et al., Eur. Phys. C **8**, 67 (1999)
107. R. Bellazzini et al., (GAMS Collaboration), Phys. Lett. B **467**, 296 (1999)
108. S. Abatzis et al., (GAMS Collaboration), Phys. Lett. B **324**, 509 (1994)
109. R.S. Longacre et al., Phys. Lett. B **177**, 223 (1986)
110. V.A. Schegelsky et al., Eur. Phys. J. A **27**, 207 (2006)
111. M. Ablikim et al., (BES Collaboration), Phys. Rev. D **72**, 092002 (2005)
112. M. Ablikim et al., (BESIII Collaboration), Phys. Rev. D **88**, 091502 (2003)
113. M. Ablikim et al., Phys. Lett. B **607**, 243 (2005)
114. M. Ablikim et al., Phys. Lett. B **642**, 441 (2006)
115. N.M. Cason et al., Phys. Rev. Lett. **48**, 1316 (1982)
116. S. Chekanov et al., Phys. Rev. Lett. **101**, 112003 (2008)
117. A.V. Anisovich et al., Phys. Rev. D **85**, 014001 (2012)
118. K.M. Ecklund et al., Phys. Rev. D **80**, 052009 (2009)
119. S. Fukui et al., Phys. Lett. B **257**, 241 (1991)
120. P. Weidenauer et al., Z Phys. C **59**, 387 (1992)
121. C. Amsler et al., Phys. Lett. B **355**, 425 (1995)
122. C. Amsler et al., Eur. Phys. J C **23**, 29 (2002)
123. D.V. Bugg, Phys. Rev. D **78**, 074023 (2008)
124. F. Antinori et al., (WA91 Collaboration), Phys. Lett. B **353**, 589 (1995)
125. M. Aguilar-Benitez, Phys. Rev. D **6**, 29 (1972)
126. J.Z. Bai et al., Phys. Rev. D **68**, 052003 (2003)
127. P. Eugenio et al., Phys. Lett. B **497**, 190 (1997)
128. K. Abe et al., (Belle Collaboration), Eur. Phys. J C **32**, 323 (2003)
129. M. Acciarri et al., (L3 Collaboration), Phys. Lett. B **501**, 173 (2001)
130. S. Uehara et al., (Belle Collaboration), Prog. Theor. Exp. Phys. 123C01 (2013)
131. S. Uehara et al., Phys. Rev. D **78**, 052004 (2008)
132. S. Uehara et al., Phys. Rev. D **82**, 114031 (2010)